JOURNAL OF BACTERIOLOGY, Dec. 2006, p. 8022–8032 Vol. 188, No. 23
0021-9193/06/$08.00+0 doi:10.1128/JB.01106-06

The Cation-Responsive Protein NhaR of *Escherichia coli* Activates *pgaABCD* Transcription, Required for Production of the Biofilm Adhesin Poly-β-1,6-*N*-Acetyl-D-Glucosamine[▽]

Carlos Goller, Xin Wang, Yoshikane Itoh, and Tony Romeo*

Department of Microbiology and Immunology, Emory University School of Medicine, Emory University School of Medicine, 3105 Rollins Research Center, 1510 Clifton Rd., N.E., Atlanta, Georgia 30322

Received 25 July 2006/Accepted 11 September 2006

The *pgaABCD* operon of *Escherichia coli* is required for production of the biofilm adhesin poly-β-1,6-*N*-acetyl-D-glucosamine (PGA). We establish here that NhaR, a DNA-binding protein of the LysR family of transcriptional regulators, activates transcription of this operon. Disruption of the *nhaR* gene decreased biofilm formation without affecting planktonic growth. PGA production was undetectable in an *nhaR* mutant strain. Expression of a *pgaA′-′lacZ* translational fusion was induced by NaCl and alkaline pH, but not by $CaCl_2$ or sucrose, in an *nhaR*-dependent fashion. Primer extension and quantitative real-time reverse transcription-PCR analyses further revealed that NhaR affects the steady-state level of *pga* mRNA. A purified recombinant NhaR protein bound specifically and with high affinity within the *pgaABCD* promoter region; one apparent binding site overlaps the −35 element, and a second site lies immediately upstream of the first. This protein was necessary and sufficient for activation of in vitro transcription from the *pgaA* promoter. These results define a novel mechanism for regulation of biofilm formation in response to environmental conditions and suggest an expanded role for NhaR in promoting bacterial survival.

Bacteria in the natural environment often form complex communities of cells associated with a surface or interface and containing a polysaccharide matrix (8, 13, 19, 30). This physiological state, known as a biofilm, provides an environment that can facilitate horizontal gene transfer and promote survival under hostile conditions (13, 15, 66). Biofilm-associated cells are generally more resistant to antimicrobial treatments than free-living bacteria (17, 24, 44). In addition, pathogenic organisms growing as biofilms are protected from attack by the immune system, and these resilient communities of microbes can lead to chronic infections (15, 24, 30, 31), resulting in medical complications and substantial economic losses (14, 47, 56). An understanding of the factors that regulate the colonization process is important for developing approaches to combat and control biofilm formation.

Biofilm development is a complex process, initiated by cell attachment to a surface and formation of microcolonies (14, 47). A temporary attachment step often precedes "permanent" attachment (2, 3, 9, 34) and may be aided by motility (53, 78). In various strains of *Escherichia coli*, attachment and microcolony formation are facilitated by proteinaceous adhesins and polysaccharides such as cellulose and poly-β-1,6-*N*-acetyl-D-glucosamine (PGA) (16, 53, 55, 58, 74, 77, 80). The latter polymer is involved in both cell-cell adhesion and attachment to certain abiotic surfaces by *E. coli* K-12, and it also stabilizes biofilm structures of other gram-negative bacteria and staphylococci (reference 36 and references therein). Its production depends upon the *pgaABCD* operon, which encodes a GT-2 family vectoral glycosyltransferase (PgaC) that synthesizes this polymer and other proteins thought to be involved in PGA export and localization. Quorum-sensing molecules and other polysaccharides influence the further maturation of various biofilms (18, 28, 52). Eventually, planktonic cells are released from the biofilm, completing the developmental cycle and leading to colonization elsewhere (47). Thus, biofilm formation may be viewed as a flexible or dynamic developmental process involving sequential gene expression patterns that are influenced by environmental cues (6, 25, 47).

Several regulatory systems affect *E. coli* biofilm formation (see, e.g., references 1, 12, 20, 37, 38, 54, and 74). The RNA-binding protein CsrA regulates biofilm formation primarily by binding to the untranslated leader and proximal coding region of *pgaABCD* mRNA, which blocks *pgaA* translation and destabilizes this transcript (37, 38, 59, 76). Thus, a *csrA* mutant overproduces PGA and exhibits a dramatic increase in biofilm formation. CsrA activity in the cell is controlled by two noncoding RNAs, CsrB and CsrC, which bind to and sequester multiple copies of CsrA and thus activate *pga* expression and biofilm formation (see, e.g., reference 76). EnvZ/OmpR, H-NS, and the Cpx and Rcs systems all appear to affect biofilm formation by regulating the production of curli fimbriae in response to osmotic conditions (16, 39, 54, 67). The Cpx system also may mediate surface sensing to activate biofilm formation (42, 48).

Living cells not only respond to changing osmotic conditions but must also maintain an externally directed sodium gradient and a relatively constant intracellular pH (51). Na^+/H^+ antiporters, membrane proteins that exchange Na^+ (or Li^+) for H^+, play important roles in these processes. In *E. coli*, NhaA is the key antiporter that protects against sodium stress, and it is essential for growth in the presence of high sodium concen-

* Corresponding author. Mailing address: Department of Microbiology and Immunology, Emory University School of Medicine, 3105 Rollins Research Center, 1510 Clifton Rd., N.E., Atlanta, GA 30322. Phone: (404) 727-3734. Fax: (404) 727-3659. E-mail: romeo@microbio.emory.edu.

▽ Published ahead of print on 22 September 2006.

TABLE 1. Strains, plasmids, and bacteriophage used in this study

Strain, plasmid, or phage	Description or genotype	Source or reference
E. coli K-12 strains		
DH5α	*supE44* Δ*lacU169* (ϕ80 *lacZ* Δ*M15*) *hsdR17 relA1 recA1 endA1 gyrA96 thi-1*	
MG1655	F^- λ^-	Michael Cashel, NICHD, National Institutes of Health, Bethesda, Maryland
TRMG	MG1655 *csrA*::*kan*	61
CF7789	MG1655 Δ*lacI-Z* (MluI)	Michael Cashel
TRCF7789	CF7789 *csrA*::*kan*	69
DJ25	TRMG Δ*motB uvrC279*::Tn*10* Δ*fimB-H*	37
XWMGDABCD	MG1655 Δ*pgaABCD*	77
TRXWMGDABCD	TRMG Δ*pgaABCD*	77
NM81	*nhaA*::*kan*	Etana Padan, Hebrew University of Jerusalem, Israel
96B10[a]	DJ25 *nhaR*::*cam* at +432 relative to initiation codon	This study
CGMR	MG *nhaR*::*cam*	This study
CGTR	TRMG *nhaR*::*cam*	This study
XWZ4	CF7789 *pgaA'-'lacZ*	76
TRXWZ4	XWZ4 *csrA*::*kan*	76
CGCFR	XWZ4 *nhaR*::*cam*	This study
CGTRCFR	TRXWZ4 *nhaR*::*cam*	This study
S. epidermidis strains		
1457	PIA positive	Dietrich Mack, Universitätsklinikum, Hamburg-Eppendorf, Germany
1457-M10	PIA negative; Ery^r $Cipro^r$ Gm^r	Dietrich Mack
Plasmids		
pKK223-3	Cloning vector; Ap^r	Pharmacia Corp.
pUC19	Cloning vector; Ap^r	
pCR 2.1 TOPO	Cloning vector; Ap^r Kn^r	Invitrogen
pCRnhaAR	*nhaAR* operon in pCR2.1	This study
pNhaR	*nhaR* in pKK223-3	This study
pNhaR-His_6	C-terminally hexahistidine-tagged NhaR for protein purification	This study
pPGA372	*pgaABCD* in pUC19	77
Bacteriophage P1vir	Strictly lytic P1	Carol Gross, University of California, San Francisco

[a] Original transposon mutant.

trations, while NhaB becomes essential only in the absence of NhaA (49, 50). The *nhaA* gene is located in a two-gene operon, *nhaAR*, which is induced by the presence of monovalent cations. The gene *nhaR* of this operon encodes an autoregulatory protein that activates *nhaAR* transcription and is homologous to the LysR-OxyR family of prokaryotic transcriptional regulators (57, 64). NhaR also activates *osmC* transcription, which is required for resistance to organic peroxides and long-term survival in stationary phase (29, 43, 68, 70).

LysR-type transcriptional regulators (LTTRs) respond to low-molecular-weight coinducer molecules, although coinducer binding often has been indirectly inferred by isolating mutants that fail to respond to, or have altered specificity for, the coinducer (64, 73, 75). Coinducers typically do not increase promoter affinity but instead activate transcription via a conformational change in the LTTR-DNA complex (11, 35, 46, 64). While NhaR activates gene expression in vivo in response to Na^+, K^+, or Li^+, this cation response has not been reconstituted in vitro (10, 22, 23, 70).

Here we establish that NhaR stimulates *pga* transcription, and thus biofilm formation, in response to monovalent cations and alkaline conditions. We propose that this represents a novel means by which NhaR promotes survival of *E. coli* and perhaps other enteric bacteria in response to environmental conditions. Despite its regulatory role in the cell, NhaR-dependent in vitro transcription did not respond to monovalent cations, suggesting that additional factors might be involved in this regulation.

MATERIALS AND METHODS

Bacterial strains, phage, plasmids, and growth conditions. All *E. coli* strains, phage, and plasmids used in the present study are listed in Table 1. Unless otherwise indicated, bacteria were routinely grown at 37°C in Luria-Bertani medium (LB) (pH 7.4) (tryptone, 10 g/liter; yeast extract, 5 g/liter; NaCl, 10 g/liter) with shaking at 250 rpm. L broth was identical to LB but lacked NaCl. Biofilms were grown in 96-well flat-bottom polystyrene microtiter plates (Corning Inc., Life Sciences, Acton, MA) at 26°C for 24 h under static conditions. Colonization factor antigen medium (1% Casamino Acids, 0.15% yeast extract, 0.005% $MgSO_4$, and 0.0005% $MnSO_4$, pH 7.4) was used for initial isolation of biofilm mutants. Media were supplemented with antibiotics as needed at the following final concentrations: ampicillin, 100 μg/ml; chloramphenicol, 25 μg/ml; kanamycin, 100 μg/ml; and tetracycline, 10 μg/ml.

Molecular biology and genetics. Standard procedures were used for isolation of supercoiled plasmids, restriction digests, ligations, transformation, and P1*vir* transduction of antibiotic markers, including *nhaR*::*cam* (45, 63).

TABLE 2. Oligonucleotide primers used in this study[a]

Primer name	Sequence (5′ to 3′)[b]	Comments
NhaAR FWD	GATTCCTCTATTTATTCGCCCGC	400 bp upstream of *nhaAR*
NhaAR REV	CACTCGTGAGCGCTTACAGCCG	3′ end of *nhaR*
NhaR FWD	AAGAATTCAACGGCTCCCTTTTCATTGTTATCAGGG	Contains upstream region of *nhaR* and EcoRI site for cloning
NhaR REV	AACTGCAGTTAACGCACCGCTGGACTAAAAAG	Contains stop codon of *nhaR* and PstI site for cloning
NhaR-His_6 REV	AACTGCAGTCAGTGGTGGTGGTGGTGGTGACGCA CCGCTGGACTAAAAAG	Contains six His codons, stop codon, and PstI site
PgaA GS FWD[c]	CAATTAAATCCGTGAGTGCCG	Anneals −115 of *pgaA*
PgaA GS REV[c]	TCTTCAGGAATACGGCATAAAT	Anneals +18 of *pgaA*
PgaB-C FWD[c]	ATCATTAATCGCATCGTATCG	Intergenic region between *pgaB* and *pgaC*
PgaB-C REV[c]	AGTGAAAGTACGCTACGCATAGGG	Intergenic region between *pgaB* and *pgaC*
PEXT3[c]	CCTCATAATCCGTTATTAAACGC	Anneals between +134 to +154 relative to the initiation of transcription of *pgaA*
PGART1	TTCTCATCATCAACAATTCACGTCTC	*pga* leader-*pgaA* forward primer
PGART2	GCGGCAGTAAGAAGTTTCAAAGC	*pga* leader-*pgaA* reverse primer
16S-4[d]	AGTTATCCCCCTCCATCAGG	16S rRNA distal, forward primer
16S-5[d]	TGCAAGTCGAACGGTAACAG	16S rRNA distal, reverse primer

[a] All primers were purchased from Integrated DNA Technologies Inc., Coralville, Iowa.
[b] Restriction sites are underlined.
[c] Primer used for gel mobility shift assays and primer extensions; primer was desalted and high-pressure liquid chromatography purified by the manufacturer.
[d] Sequence was previously published (27).

Quantitative biofilm assay. Biofilm formation was assayed by crystal violet staining of adherent cells in microtiter wells, as described previously (38). Overnight cultures were diluted 1:100 into fresh LB without antibiotics or supplemented with ampicillin for strains harboring a plasmid. Bacterial growth was determined by measuring the absorbance at 600 nm using a Synergy-HT plate reader (BioTek, Winooski, VT) prior to crystal violet staining. At least 16 replicates were conducted for each sample, and each experiment was performed at least twice. The results were calculated as averages and standard errors of the means, using the GraphPad Prism software package (San Diego, CA). Tukey's multiple-comparison test was used for statistical analysis of data (GraphPad Prism).

Detection of PGA. Overnight cultures were diluted 1:100 into fresh LB. Cultures were incubated for 24 h at 26°C with shaking at 250 rpm and were harvested (10 ml) and resuspended in 400 μl of a solution containing 50 mM Tris-HCl (pH 8.0), 10 mM EDTA, and 1 μg lysozyme. After incubation at room temperature for 30 min, a solution (300 μl) containing 10 μg DNase I, 40 μg RNase, 200 μg α-amylase, and 40 mM $MgCl_2$ was added. The mixture was incubated at room temperature for 1 h with occasional mixing before being heated to 37°C for 2 h. The resulting cell lysate was then extracted once with 50 mM Tris (pH 8.0)-saturated phenol and once with chloroform. The aqueous phase (1 ml from 10 ml of culture) was collected, and residual chloroform was allowed to evaporate overnight at room temperature. The samples were concentrated using a YM-3 membrane (Amicon, Houston, TX; molecular mass cutoff, 3,000 Da).

For cell-bound PGA, 3 μl of sample, corresponding to 1 ml of the culture, was applied onto a nitrocellulose membrane and allowed to air dry overnight at room temperature. For PGA from spent medium, 3 μl of sample, corresponding to 75 μl of culture, was used. The membrane was blocked for 1 h in 5% nonfat dry milk in PBS-T (1.47 mM NaH_2PO_4, 8.09 mM Na_2HPO_4, 0.145 mM NaCl, and 0.5% Tween 20). A primary antistaphylococcal polysaccharide intercellular adhesin (PIA) (poly-β-1,6-*N*-acetyl-D-glucosamine) rabbit antiserum was used at a dilution of 1:5,000 in 1% bovine serum albumin–PBS-T for 1 h. This antiserum was a generous gift from Dietrich Mack (33, 62). After the membrane was washed twice for 5 min and twice for 10 min with PBS-T, the secondary horseradish peroxidase-conjugated antibody (1:10,000; Sigma-Aldrich) was applied for 1 h. The membrane was then washed, and the signal was detected by chemiluminescence, as recommended by the manufacturer (Western Lightning Plus protocol; Perkin-Elmer). Membranes were photographed using a Bio-Rad ChemiDoc system. The complete experiment was conducted twice with essentially identical results. PIA-positive and -negative strains (*Staphylococcus epidermidis* 1457 and 1457-M10, respectively) were used as controls.

Plasmid construction. Enzymes for molecular cloning were purchased from Promega (Madison, WI) or New England Biolabs (Ipswich, MA). Constructs were electroporated into DH5α cells, and recombinant plasmids were isolated using QIAGEN (Valencia, CA) reagents. Cloned inserts were determined to be free of mutations by DNA sequencing.

Molecular cloning of the *nhaAR* operon involved PCR amplification of chromosomal DNA with the primers NhaAR FWD and NhaAR REV (Table 2) and Elongase (Invitrogen, Carlsbad, CA) under the reaction conditions described by the manufacturer. Annealing temperatures and extension times were based on primer melting temperature and final product size, respectively. The 2.4-kb product was cloned into pCR 2.1 TOPO (Invitrogen).

The *nhaR* gene was amplified from pCRnhaAR plasmid DNA by using Elongase and the primers NhaR FWD and NhaR REV (Table 2). The 940-bp PCR product and pKK223-3 were each digested with EcoRI and PstI, gel purified using the QIAGEN gel extraction kit, and ligated to create pNhaR.

A C-terminally His-tagged *nhaR* gene was amplified from pCRnhaAR by using *Pfu* Turbo DNA polymerase (Stratagene) as indicated by the manufacturer, with primers NhaR FWD and NhaR-His_6 REV (Table 2). The pNhaR-His_6 plasmid was constructed using the procedures described for pNhaR and was confirmed to complement the *nhaR* mutant phenotype in vivo.

β-Galactosidase and total protein assays. β-Galactosidase activity was assayed as described previously (60), except that activities of *csrA* wild-type and mutant strains were determined with 2-h and 1-h reaction times, respectively, and expressed as activity per hour. Cultures were grown at 26°C in LB with shaking, and 500 μl of cells was concentrated and used for each assay. Reactions were performed in triplicate. Total cellular protein was measured by the bicinchoninic acid method (BCA protein assay; Pierce, Rockford, IL) using bovine serum albumin as the standard (65). Absorbance measurements were conducted in flat-bottom 96-well microtiter plates with a Synergy HT plate reader (BioTek).

Isolation of total RNA. Total cellular RNA was prepared using the MasterPure RNA purification kit (Epicenter, Madison, WI). DNA was removed from the preparations that were to be analyzed by quantitative real-time reverse transcription-PCR (q-RT-PCR), using two DNase I digestion steps, as recommended (Epicenter). RNA was quantified by its absorbance at 260 and 280 nm, and rRNA integrity was assessed on formaldehyde-agarose gels. RNA samples were stored at −80°C in 70% ethanol.

Primer extension analysis. Primer extension analyses were performed according to the protocol of Wang et al. (76). Cells were grown in LB at 26°C to the transition to stationary phase of growth and harvested, and total RNA was prepared. A primer, PEXT3, that anneals between positions 134 and 154 relative to the transcript initiation site of *pgaABCD* was 5′ end labeled with [γ-^{32}P]ATP (3,000 Ci/mmol; Perkin-Elmer, Boston, MA) by using T4 polynucleotide kinase (Promega), as described in the manufacturer's manual. Unincorporated [γ-^{32}P]ATP was removed using MicroSpin G-25 columns (Amersham Biosciences, Piscataway, NJ). Labeled primer (~6 pmol) was added to 40 μg of total RNA. Reverse transcription was performed for 60 min at 50°C using the ThermoScript RT-PCR system (Invitrogen), according to the manufacturer's instructions. The labeled primer and a plasmid template (pPGA372) were used to generate a corresponding DNA sequencing ladder with the SequiTherm EXCEL II DNA sequencing kit (Epicenter). The primer extension products were ana-

lyzed on a 6% polyacrylamide sequencing gel containing 6 M urea, which was dried and subjected to autoradiography using a phosphorimager (Storm 860; Amersham Bioscience). Two different concentrations of RNA were examined to ensure that the signal was limited by the RNA transcripts and not the primer concentration.

q-RT-PCR analysis of *pgaA* mRNA. For q-RT-PCR, *csrA* wild-type (MG1655) and mutant (TRMG) strains containing a wild-type or mutant *nhaR* gene were grown at 26°C in LB to transition phase. Total RNA was isolated and treated to remove DNA, and the steady level of *pgaL-A* was determined with the primer pair PGART1/PGART2 (Table 2), using the iScript one-step RT-PCR Kit with SYBR green (Bio-Rad, Hercules, CA) according to the manufacturer's guidelines. Reactions were performed in duplicate using 100 ng RNA template. A reaction lacking reverse transcriptase was included for each sample as a control for DNA contamination. Reactions were conducted using the iCycler iQ real-time system (Bio-Rad) under the following conditions: 65°C for 5 min; 53°C for 60 min; 95°C for 10 min, and 35 cycles of 95°C for 30 s, 57°C for 1 min, and 68°C for 1 min. The difference in cycle threshold between samples from wild-type and mutant strain pairs was calculated. The PCR product identities were confirmed by agarose gel electrophoresis, and product uniformity was determined using melting curves (iCycler instruction manual; Bio-Rad). These experiments were conducted three times with similar results, and the mean values from the three experiments were determined. A standard curve for each experiment was constructed using a plasmid template to ensure linearity of the reactions under our experimental conditions. For normalization of *pgaA* RNA levels, the primer pair 16S-4/16S-5 (Table 2) was used to amplify 99 bp of 16S rRNA, using 1- and 10-ng samples of total RNA and a 20-min reverse transcription time.

Purification of NhaR-His$_6$. NhaR-His$_6$ was purified as described previously, with some modification (10). An overnight culture of *E. coli* DH5α(pNhaR-His$_6$) was used (20 ml/liter) to inoculate 1 liter of LB, and the culture was grown at 37°C with aeration to an A_{600} of 0.6. Isopropyl-β-D-thiogalactopyranoside (IPTG) (2 mM) was added to the culture, and growth was continued for 3 h before cells were harvested by centrifugation and stored at −80°C. Frozen cells were thawed and resuspended (2 g of cells per ml) in lysis buffer containing 1 mg/ml of lysozyme, 4 mM imidazole, 20 mM Tris-HCl (pH 7.9), 500 mM KCl, and 5 mM β-mercaptoethanol (BME). After incubation on ice for 30 min, cells were disrupted by sonication. NhaR-His$_6$ was then purified by affinity chromatography using a His-Trap column (QIAexpressionist; QIAGEN), as recommended by the manufacturer. The binding buffer consisted of 4 mM imidazole, 500 mM KCl, 20 mM Tris-HCl (pH 7.9), and 5 mM BME. Wash and elution buffers were identical to binding buffer except that they contained 60 and 400 mM imidazole, respectively. This single chromatographic step provided an almost homogeneous preparation of NhaR-His$_6$ with greater than 98% purity, as assessed by sodium dodecyl sulfate-polyacrylamide gel electrophoresis with Coomassie blue staining. Fractions containing the peak concentration of NhaR-His$_6$ were pooled and dialyzed overnight at 4°C against 20 mM Tris-HCl (pH 7.9), 50 mM KCl, 1 mM EDTA (pH 8.0), 15 mM BME, and 10% glycerol. Glycerol was added to 10%, and aliquots (100 μl) were stored at −80°C. This procedure yielded ~0.54 mg of His-tagged NhaR per liter of culture. For experiments designed to examine cation dependency, the protein was extensively dialyzed against this buffer lacking the KCl.

MALDI-TOF mass spectrometry. NhaR-His$_6$ was confirmed by matrix-assisted laser desorption ionization–time-of-flight (MALDI-TOF) mass spectrometry. Spectra were acquired in a linear mode by using a Voyager STR (Applied Biosystems, Foster City, CA) and a nitrogen laser (λ = 337 nm). One hundred to 600 laser pulses were used to obtain the spectra. The matrix was a saturated solution of 1,4-hydroxyphenylazobenzoic acid in 50% acetonitrile and 1% trifluoroacetic acid and was mixed in a 10:1 ratio with sample. One microliter of the mixture was transferred to the sample plate and allowed to dry. The predicted mass of recombinant NhaR-His$_6$ is 35,110 Da, and the experimental mass was determined to be 35,168 Da. The Voyager MALDI-TOF mass spectrometer with internal calibration is sensitive to ±0.05% (±20 Da). The larger experimental mass was suggestive of a K^+ (40-Da) ion associated with the protein.

Gel mobility shift assay with purified NhaR-His$_6$ and DIG-labeled *pga* DNA. A 132-bp PCR product containing the promoter region of *pgaABCD* was amplified using primers PgaA GS FWD and PgaA GS REV (−115 to +18) (Table 2) and *Taq* polymerase (Promega). This product was 3′ end labeled with digoxigenin (DIG)-11-ddUTP (DIG gel shift kit, second generation; Roche Diagnostics, Indianapolis, IN) as suggested by the manufacturer. Purified recombinant NhaR (NhaR-His$_6$, 1.17 μM) was added to DNA binding reaction mixtures (10 μl) containing 50 mM KCl, 20 mM Tris-HCl, (pH 7.9), 1 mM dithiothreitol, 10% glycerol, 125 μg/ml bovine serum albumin, and 1.38 fmol of DIG-labeled PCR product. Reactions were carried out for 20 min at 25°C. Loading dye (1.6 μl) containing bromophenol blue and glycerol, supplied with the labeling kit (Roche Diagnostics), was immediately added and gently mixed, and reactions were subjected to native gel electrophoresis (5% acrylamide, 0.5× TBE [50 mM Tris, 40 mM boric acid, 0.5 mM EDTA]) at room temperature. The DNA was electroblotted (400 mA, 12 V, 45 min) onto positively charged nitrocellulose membranes (Roche Diagnostics). Membranes were rinsed for 10 min in 2× SSC (1× SSC is 0.15 M NaCl plus 0.015 M sodium citrate), and nucleic acids were cross-linked (UV Stratalinker 1800; Stratagene, La Jolla, CA). The signal was detected by chemiluminescence as recommended by the manufacturer (Wash and Block buffer set; Roche Diagnostics), using a Bio-Rad ChemiDoc system.

A nonspecific control DNA (*pgaB-C*) with a size and G+C content similar to those of the promoter DNA was amplified from the region overlapping *pgaB* and *pgaC* by using the primer set PgaB-C FWD/PgaB-C REV (Table 2). Quantity One (Bio-Rad) software was used to analyze the blots and quantify the bound and unbound probe. An apparent equilibrium binding constant (K_d) for the NhaR-*pgaA* DNA complex was calculated using GraphPad Prism (Graph Pad) according to a previously described cooperative binding equation (79), adapted as follows: $pgaA_b = Y_{max} \times [(NhaR_f/K_d)^n]/\{1 + [(NhaR_f/K_d)^n]\}$. In this equation, Y_{max} is the maximum possible bound fraction (100%) of *pgaA* probe DNA ($pgaA_b$), and K_d is the concentration of free protein ($NhaR_f$) at which $pgaA_b$ reaches 50% bound. Isolated NhaR protein was assumed to be 100% active for the calculations. The cooperativity of binding is described by the Hill coefficient (n).

DNase I footprint of NhaR-His$_6$ on a linear DNA fragment of *pgaA*. Oligonucleotides PgaA GS FWD and PgaA GS REV (100 pmol) were individually end labeled with [γ-^{32}P]ATP (6,000 Ci/mmol; Perkin-Elmer) using T4 polynucleotide kinase (Epicenter) as per the manufacturer's instructions. Each labeled primer (20 pmol) was then used with the corresponding unlabeled primer (20 pmol) to amplify the promoter region of the *pgaABCD* operon from pPGA372 plasmid DNA with Platinum *Taq* polymerase (Invitrogen). The final PCR products corresponded to a 132-bp fragment containing the promoter region of *pgaA* (−115 to +18) and were gel purified and cleaned with QIAGEN QuickSpin columns.

Footprinting reaction mixtures contained 0.67 pmol (≥10,000 cpm) of the end-labeled DNA and were incubated with increasing concentrations of NhaR-His$_6$. The 20-μl reaction mixtures contained 33 mM Tris acetate (pH 8.0), 0.15 mg/ml bovine serum albumin, 10 mM Mg acetate, 1 mM dithiothreitol, and 10% glycerol. The reaction mixtures were incubated at 25°C for 15 min before addition of DNase I (2 μl of a 0.01-mg/ml solution; 51.8 units). After 5 min at 25°C, the digests were terminated by addition of 200 μl of stop buffer (570 mM ammonium acetate, 80% ethanol). The DNA in each reaction was precipitated with ethanol, using Pellet Paint coprecipitant (Novagen, San Diego, CA). The same labeled primer and plasmid template pPGA372 were used to generate a DNA sequencing ladder with the SequiTherm EXCEL II DNA sequencing kit (Epicenter). Products were separated on 6 M urea–8%polyacrylamide sequencing gels. Gels were dried under vacuum, and the labeled fragments were detected using a Storm 860 phosphorimager (Amersham Bioscience). Footprinting reactions were conducted in the presence or absence of added sodium chloride. The experiment was conducted four times.

In vitro transcription. For in vitro transcription reactions, supercoiled plasmid pPGA372 (1 μg) and His-tagged NhaR (455 nM) were mixed in a 50-μl reaction mixture containing 50 mM Tris-HCl (pH 8.0), 10 mM $MgCl_2$, 1 mM dithiothreitol, and 10% glycerol and incubated at 25°C for 20 min. *E. coli* σ^{70}-RNA polymerase holoenzyme (1.25 U; Sigma-Aldrich Corp., St. Louis, MO) was added, and the mixtures were incubated for 10 min at 37°C. For transcription, 3.5 μl of a mixture of the four nucleoside triphosphates (2.5 mM each) and 40 U of Superasin RNase inhibitor (Ambion, Austin, TX) was added, and the solution was incubated for 30 min at 37°C. The potassium and sodium contents of the reaction mixtures were estimated to be no greater than 1.1 mM. Transcription reactions were terminated by incubation with DNase I (5 units; Epicenter) for 15 min. The mixtures were extracted twice with phenol-chloroform and three times with chloroform, and RNA was precipitated with ethanol and resuspended in diethylpyrocarbonate-treated water (10 μl).

The *pgaA* transcript was detected by primer extension. PEXT3-labeled primer (3.5 pmol) was added to in vitro-transcribed RNA (5 μl). For comparison, total RNA (25 μg) from the indicated strains was analyzed as stated above (see "Primer extension analysis"), except that Superasin (Ambion) was added to the reaction mixture instead of the RNase inhibitor supplied with the reverse transcriptase.

Microscopy. Sterile borosilicate coverslips were placed in 15-cm petri dishes containing 25 ml of a freshly inoculated (1:100) overnight culture. The petri dishes were incubated at room temperature, and coverslips were removed at various times and rinsed gently with water. Each coverslip was inverted over a Parafilm gasket on a microscope slide, and images were obtained 10 min thereafter, as described previously (2, 3). Adherent cells were viewed by transmitted

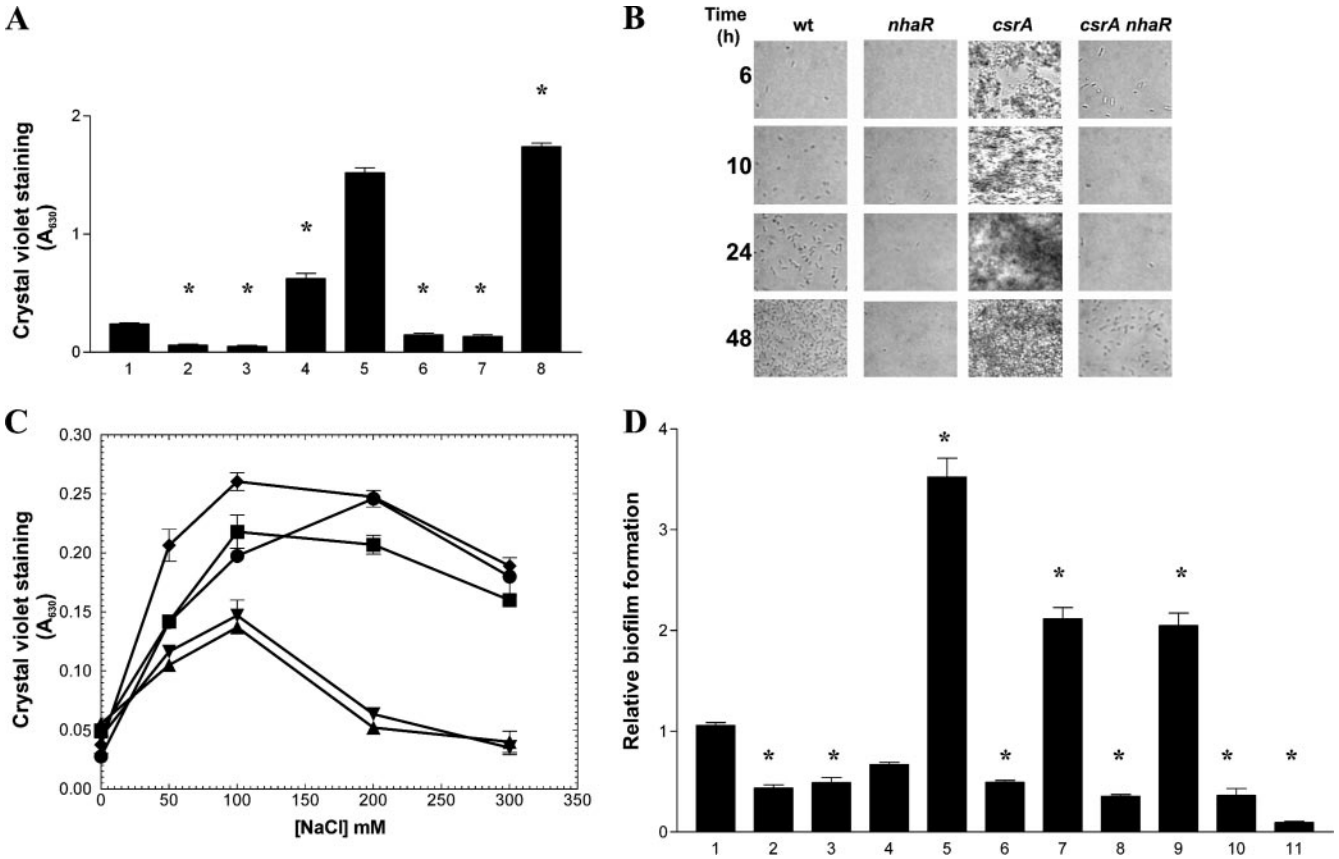

FIG. 1. Disruption of *nhaR* of *E. coli* affects biofilm formation. (A) Cultures were grown in microtiter plates in LB (pH 7.4) for 24 h at 26°C, and biofilm formation was assessed by crystal violet staining (see Materials and Methods). Bars depict the results obtained with a series of isogenic strains: 1, MG1655 (wild type); 2, *nhaR*::*cam*; 3, *nhaR*::*cam*(pKK223-3); 4, *nhaR*::*cam*(pNhaR); 5, *csrA*::*kan*; 6, *csrA*::*kan nhaR*::*cam*; 7, *csrA*::*kan nhaR*::*cam*(pKK223-3); 8, *csrA*::*kan nhaR*::*cam*(pNhaR). Error bars indicate standard errors of the means. (B) Time course of adherence to coverslips by isogenic *E. coli* K-12 MG1655 strains (described in Materials and Methods). Representative fields are shown. wt, wild type. (C) Effect of sodium chloride on biofilm formation. Cultures were grown in L broth (LB without NaCl) supplemented with the indicated concentrations of NaCl. Symbols represent the results obtained with a series of isogenic strains: ■, MG1655 (wild type); ▲, *nhaR*::*cam*; ▼, *nhaR*::*cam*(pKK223-3); ◆, *nhaR*::*cam*(pNhaR); ●, *nhaR*::*cam*(pNhaR-His_6). Bars represent the averages for two wells, and error bars correspond to the standard errors of the means. (D) Epistasis analyses of *nhaR* and *pgaABCD* on biofilm formation. Biofilm formation in the following isogenic strains was assessed as for panel A: 1, MG1655; 2, Δ*pgaABCD*; 3, *nhaR*::*cam*; 4, MG1655(pUC19); 5, MG1655(pPGA372) (contains *pgaABCD*); 6, *nhaR*::*cam*(pUC19); 7, *nhaR*::*cam*(pPGA372); 8, Δ*pgaABCD*(pUC19); 9, Δ*pgaABCD*(pPGA372); 10, Δ*pgaABCD*(pKK223-3); 11, Δ*pgaABCD*(pNhaR). Bars represent the averages for 16 wells normalized to the biofilm formed by MG1655, and error bars correspond to the standard errors of the means. The asterisks denote significant differences relative to the corresponding parent strain ($P < 0.001$ [Tukey's multiple-comparison test]).

light with an Olympus 1X71 microscope (40× objective lens with a 1.6× selector; Olympus, Thornwood, NY). The images were captured by using a charge-coupled device camera (COHU-4915; COHU, Inc., Florence, KY) connected to a frame-grabber board installed in a personal computer and processed using Image Pro-Plus 4.5 software (Media Cybernetics, Silver Spring, MD).

Bioinformatics. The phylogenetic distribution of NhaR was assessed using BLAST analyses (4) at the NCBI website, using the *E. coli* protein as the query sequence.

RESULTS AND DISCUSSION

***nhaR* is needed for optimal biofilm formation.** In order to identify genes that affect biofilm formation in *E. coli* K-12 (DJ25), Wang et al. conducted a random transposon mutagenesis and screened for altered biofilm phenotypes (77). This screen yielded an insertion in the *nhaR* open reading frame (*nhaR*::*cam*), which was determined by transduction to be linked to the biofilm-deficient phenotype of this strain (96B10). The gene product of *nhaR* is a 301-amino-acid DNA-binding protein of the LysR family, which is involved in adaptation to elevated Na^+ and alkaline pH and activates expression of the *nhaAR* operon (10, 22, 49, 57). Transduction of the *nhaR*::*cam* mutation into both MG1655 and its isogenic *csrA*::*kan* mutant caused growth inhibition under the combination of high sodium (0.6 M NaCl) and high pH (8.5) on solid media, but growth was normal on LB. The growth defect was restored by complementation with pNhaR, a plasmid clone of *nhaR* (data not shown). The *nhaR* mutant exhibited normal motility (data not shown).

Disruption of *nhaR* significantly decreased biofilm formation in both MG1655 (4-fold) (Fig. 1A, compare bars 1 and 2) and its isogenic *csrA* mutant (>10-fold) (compare bars 5 and 6). A plasmid containing *nhaR* (pNhaR) complemented the biofilm defect of *nhaR*::*cam* mutants (Fig. 1A and data not shown), confirming the role of this gene in biofilm formation. In fact, this plasmid enhanced biofilm formation beyond that formed

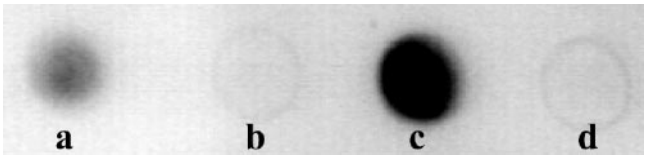

FIG. 2. Effect of *nhaR* mutation on accumulation of PGA. Cell lysates were prepared from a series of isogenic strains and analyzed by immunoblotting with an anti-PIA antiserum (see Materials and Methods). Sample identities are as follows: (a) parent (TRMG); (b) *nhaR*::*cam*; (c) *nhaR*::*cam*(pNhaR); (d) Δ*pgaABCD*. This experiment was repeated in entirety three times, with essentially identical results. A representative blot is shown.

by the wild-type strain (Fig. 1A, compare bars 1 and 4). Disruption of *nhaR* also compromised the ability of these strains to adhere to borosilicate glass coverslips, even after 60 h of incubation (Fig. 1B and data not shown), demonstrating that these mutants are not simply delayed in biofilm development. Multilayered biofilms were not formed by *nhaR* mutants, and these strains were defective in making the transition from temporary to permanent attachment (data not shown), as described previously (2). Consistent with the known response of NhaR to sodium levels, biofilm formation in MG1655 was inducible (~5-fold) by the addition of NaCl (100 mM) to L broth (Fig. 1C). The *nhaR* mutant showed more modest effects (~2.5-fold), which were complemented in *trans* by pNhaR or a similar plasmid expressing a hexahistidine-tagged NhaR protein (Fig. 1C). Because *nhaR* was expressed from a *tac* promoter in the latter example, it is clear that activation via NaCl does not simply reflect increased *nhaAR* expression by this autoregulatory protein. This *nhaR* mutation caused strains to become defective for biofilm formation at 26°C or 37°C in colonization factor antigen medium, in unbuffered LB, or in LB buffered to pH 6.4, 7.4, or 8.4 (data not shown). The altered attachment behavior of the *nhaR* mutant was similar to that of *pga* mutants, which do not produce the polysaccharide adhesin PGA (2, 77).

Regulation of biofilm formation by NhaR depends on the *pgaABCD* operon. Next, we conducted experiments to gain insight into the mechanism by which NhaR affects biofilm formation. Plasmidic expression of *nhaR* in an *nhaA* mutant strain increased biofilm, establishing that NhaR effects on biofilm were mediated independently of the Na^+/H^+ antiporter NhaA (data not shown). The biofilm defect of an *nhaR* mutant was restored by ectopic expression of *pgaABCD* from a multicopy plasmid (Fig. 1D, compare bars 3 and 7). However, biofilm formation in a strain with the *pgaABCD* operon deleted was not affected by ectopic expression of *nhaR* (data not shown). These results are consistent with the possibility that *nhaR* might be needed for the production of PGA.

An *nhaR* mutant does not accumulate PGA. To examine the effect of NhaR on PGA accumulation, relative levels of cell-bound PGA were compared by immunoblot analysis of *nhaR* wild-type and isogenic mutant strains, as well as a control strain with *pgaABCD* deleted. Parental and complemented *nhaR* mutant strains (Fig. 2a and c, respectively) produced anti-PIA-reacting material, whereas *nhaR*::*cam* and Δ*pgaABCD* mutants failed to react with the antiserum (Fig. 2b and d, respectively).

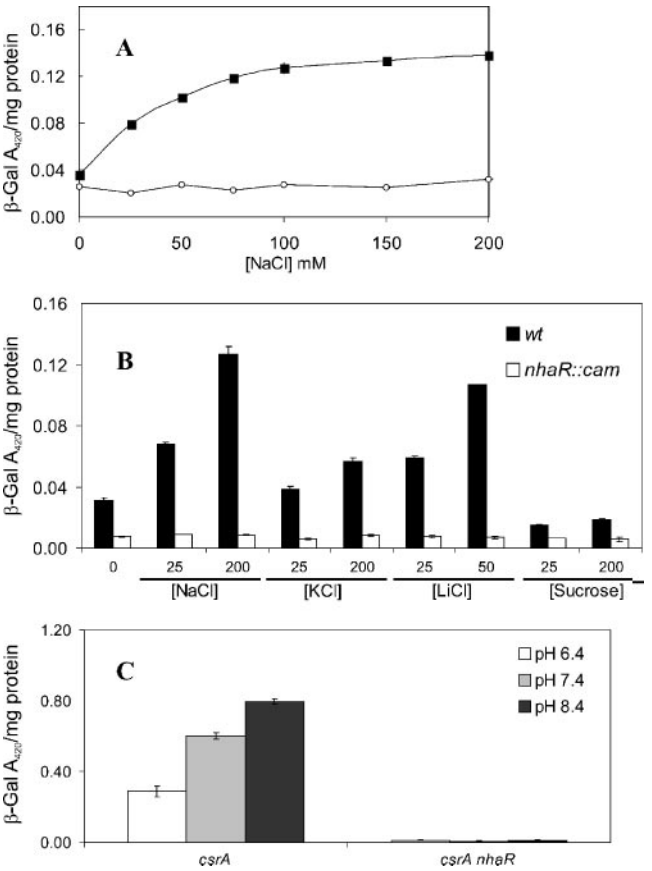

FIG. 3. Effects of *nhaR*::*cam*, monovalent cations and pH on expression of a *pgaA′-′lacZ* translational fusion. (A) Activity of the *pgaA′-′lacZ* chromosomal fusion in XWZ4 (■) and its isogenic *nhaR* mutant (CGCFR) (□) after 14 h of growth at 26°C in L broth (LB without NaCl) or in L broth supplemented with the indicated concentrations of NaCl. (B) Activity of the reporter fusion in L broth containing the indicated concentrations (mM) of NaCl, KCl, LiCl, or sucrose. wt, wild type. (C) Effect of pH on *pgaA′-′lacZ* expression. Strains were grown for 24 h at 26°C in LB buffered with 60 mM 1,3-bis[tris(hydroxymethyl)-methylamino]propane, and the pH was adjusted to the indicated values with HCl. Values represent the means for three separate reactions ± standard errors of the means. Error bars smaller than the symbols are not visible. These experiments were repeated at least three times with similar results.

In addition, disruption of *nhaR* prevented the accumulation of PGA in the culture supernatant (data not shown).

NhaR is required for induction of *pgaA′-′lacZ* expression by monovalent cations and alkaline pH. To test whether NhaR regulates the *pgaABCD* operon itself, expression of a chromosomally carried *pgaA′-′lacZ* translational fusion containing the upstream noncoding region through the initiation codon of *pgaA* (76) was examined in *nhaR* wild-type and mutant strains. This reporter fusion was activated by increasing concentrations of NaCl in the *nhaR* wild-type strain but not in the isogenic mutant (Fig. 3A).

Previously, NhaR was found to activate gene expression in response to increasing [NaCl], [KCl], [LiCl], or pH of the medium (23, 70). We found that increasing [NaCl], [LiCl], and alkaline pH also activated expression of *pgaA′-′lacZ* in an *nhaR*-dependent fashion (Fig. 3B and C). Addition of KCl or

$MgCl_2$ at the same osmolarity as NaCl weakly induced *pgaA′-′lacZ* expression, whereas sucrose or $CaCl_2$ did not (Fig. 3B and data not shown), suggesting that this response is not due to increasing osmolarity or Cl^- concentration.

Previous studies indicated that transcription of *nhaAR* in *E. coli* increases as the pH of the medium is increased from 6.5 to 8.5 (22). Furthermore, exposure of *Shewanella oneidensis* to alkaline pH caused upregulation of *nhaA* and *nhaR* transcripts (41). Thus, we grew cultures at pH 6.4, 7.4, and 8.4 in LB buffered with 60 mM 1,3-bis[tris(hydroxymethyl)-methylamino]-propane-HCl (22) and examined the expression of the *pgaA′-′lacZ* fusion. This expression increased from pH 6.4 up to 8.4 in a *csrA* mutant strain and was virtually eliminated by disruption of *nhaR* (Fig. 3C). Biofilm formation in the strain increased modestly from pH 6.4 to 7.4 but, in contrast to *pgaA′-′lacZ* expression, decreased slightly in medium at pH 8.4 (data not shown). In *csrA* wild-type strains, expression of the fusion also increased modestly from pH 6.4 to 7.4 and then decreased modestly at pH 8.4, more closely reflecting the results of biofilm assays in this strain (data not shown). Expression of *csrA′-′lacZ* and *csrB-lacZ* fusions did not vary substantially at these pH levels (data not shown). This suggests that the *csrA* and *csrB* genes, which posttranscriptionally control *pgaABCD* expression, were not responsible for the effects of pH on the *pgaABCD* operon.

Examination of other possible influences on *pga* expression. H-NS regulates many stress response genes by acting as a major component of chromatin and by responding to changes in osmolarity (5, 21). Furthermore, *hns* mutants are derepressed for *nhaAR* expression (22). We observed that *pgaA′-′lacZ* expression was only slightly increased (25 to 30%) and was still inducible by NaCl in an *hns* mutant strain background (data not shown), suggesting that HN-S is not a major regulatory determinant of *pga* gene expression. Mutations eliminating the stationary-phase sigma factor RpoS and the response regulator OmpR did not affect *pgaA′-′lacZ* expression (data not shown). However, OmpR modestly activates biofilm formation in these strains (reference 38 and data not shown). Thus, the modest induction of biofilm formation by NaCl in an *nhaR* mutant (Fig. 1C) may be due to the effect of OmpR. A transposon insertion that was isolated during the course of these studies in the *rcsD* (*yojN*) gene of the RcsC-RcsD-RcsB signal transduction system affected biofilm formation but not *pgaA′-′lacZ* expression (data not shown), indicating that the Rcs regulatory system, which responds to osmolarity and envelope stress, does not affect *pga* expression. In addition, we previously determined that *cpxR* does not affect biofilm formation by MG1655 or its isogenic *csrA* mutant (3).

***nhaR* affects *pga* transcript levels in vivo.** Our previous studies revealed that (i) the *pgaABCD* genes are cotranscribed as an operon, (ii) the 5′ end of the *pgaABCD* transcript corresponds to an A residue 234 nucleotides upstream from the *pgaA* initiation codon, and (iii) all four coding regions of this transcript are elevated in a *csrA* mutant (76). Primer extension analysis (Fig. 4, compare lanes 1 and 5) further demonstrated that this transcript was absent from *nhaR* mutants (lanes 2, 3, 6, and 7) and was restored upon complementation by a multicopy plasmid clone of *nhaR* (lanes 4 and 8). *pga* transcript levels were positively correlated with the amounts of biofilm formed by these strains (Fig. 4 and 1A and data not shown).

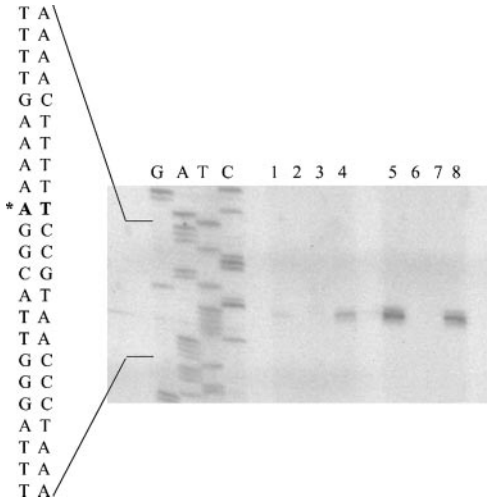

FIG. 4. Primer extension analysis of *pgaA* transcript in *nhaR* wild-type and mutant (*nhaR*::*cam*) strains. Cultures were grown at 26°C with shaking and harvested for RNA isolation in the late exponential phase of growth. Strain identities are as shown in Fig. 1A. The dideoxy sequencing ladder (lanes G, A, T, and C) was generated with PEXT3, using pPGA372 as a template. The 5′ end of the *pgaA* transcript is marked with an asterisk.

q-RT-PCR was used to quantitate the effect of *nhaR* on steady-state levels of the *pgaA* transcript (see Materials and Methods). Disruption of *nhaR* decreased *pgaA* transcript levels 200-fold in both the *csrA* wild-type and mutant backgrounds.

Purified recombinant NhaR binds specifically to *pgaABCD* promoter DNA. To determine whether NhaR-His_6 binds to *pgaA* promoter DNA, gel mobility shift assays were conducted using a 132-bp labeled DNA fragment containing the promoter region and putative NhaR binding sites of *pgaA*. Binding produced a single shift with an apparent K_d of 0.21 μM (Fig. 5), which is within the range of at least one other LTTR (7). The Hill coefficient was determined to be 1.28 ± 0.17, suggesting that the binding might be weakly cooperative. Binding was not affected by the presence or absence of 50 and 100 mM NaCl, KCl, or LiCl in the reaction mixtures (data not shown). Competition studies confirmed the specificity of this binding (Fig. 5B).

LTTRs generally bind degenerate inverted repeats that have a T-N_{11}-A motif and are found upstream of −35 promoter elements (64). Comparison of the putative *pgaABCD* promoter region with NhaR binding sites of *nhaA* (10) and *osmC* (68) revealed two T-N_{11}-A motifs, one overlapping the −35 promoter element and a second further upstream (Fig. 6E and data not shown).

DNase I footprinting of NhaR binding to *pgaA* promoter DNA. To more precisely define the NhaR binding sites on the *pgaA* promoter, DNase I footprint analysis was conducted with NhaR-His_6 and a DNA fragment (from −115 to +18 with respect to the 5′ end of the *pga* transcript). NhaR protected a region spanning ~60 bp which overlapped and extended upstream from the putative −35 promoter region (Fig. 6). Within this protected region, two apparent binding sites with dyad symmetry were separated by a small region that became hypersensitive to DNase I digestion in the presence of NhaR, suggestive of an altered conformation. The extended region of

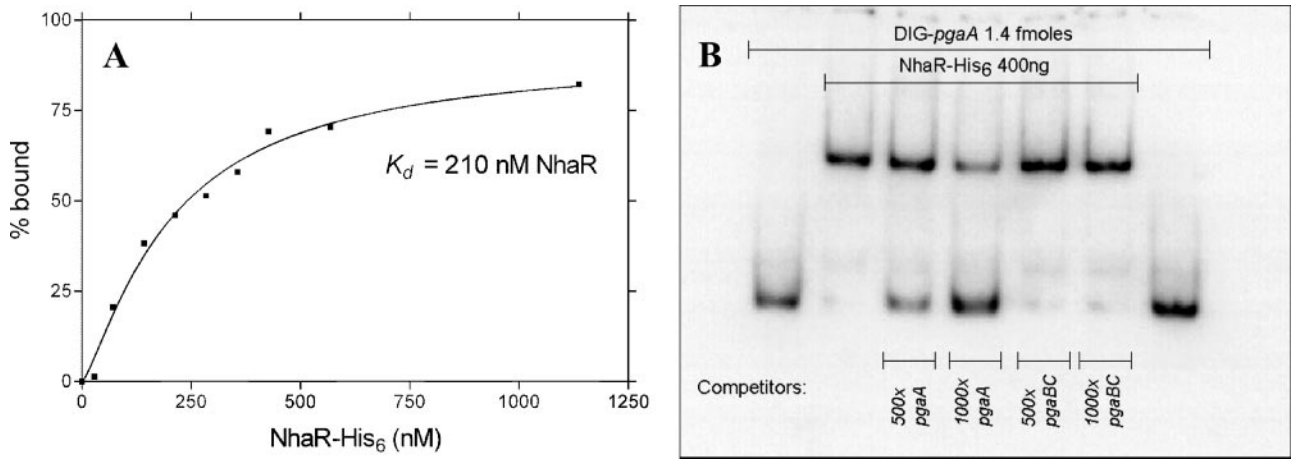

FIG. 5. Purified NhaR-His$_6$ binds specifically to *pgaABCD* promoter DNA. (A) A 132-bp PCR product containing the promoter region and putative NhaR binding site of *pgaA* was 3′ labeled with DIG-11-ddUTP and used for gel mobility shift assays. The apparent equilibrium binding constant (K_d) was determined as described in Materials and Methods. (B) Five hundred- and 1,000-fold molar excesses of unlabeled specific DNA (*pgaA*) and nonspecific DNA (*pgaBC*) were used as competitors in the binding reactions.

protection was seen on both strands and is characteristic of LysR-type transcriptional regulators (11, 64, 72). In addition, a hypersensitive region immediately downstream of the −10 element also became evident in the presence of NhaR. Addition of 50 mM NaCl had no consistent effect on the footprint (compare Fig. 6A and C and Fig. 6B and D).

NhaR is required for in vitro transcription of *pgaABCD*. To further examine the role of NhaR in *pga* expression, in vitro

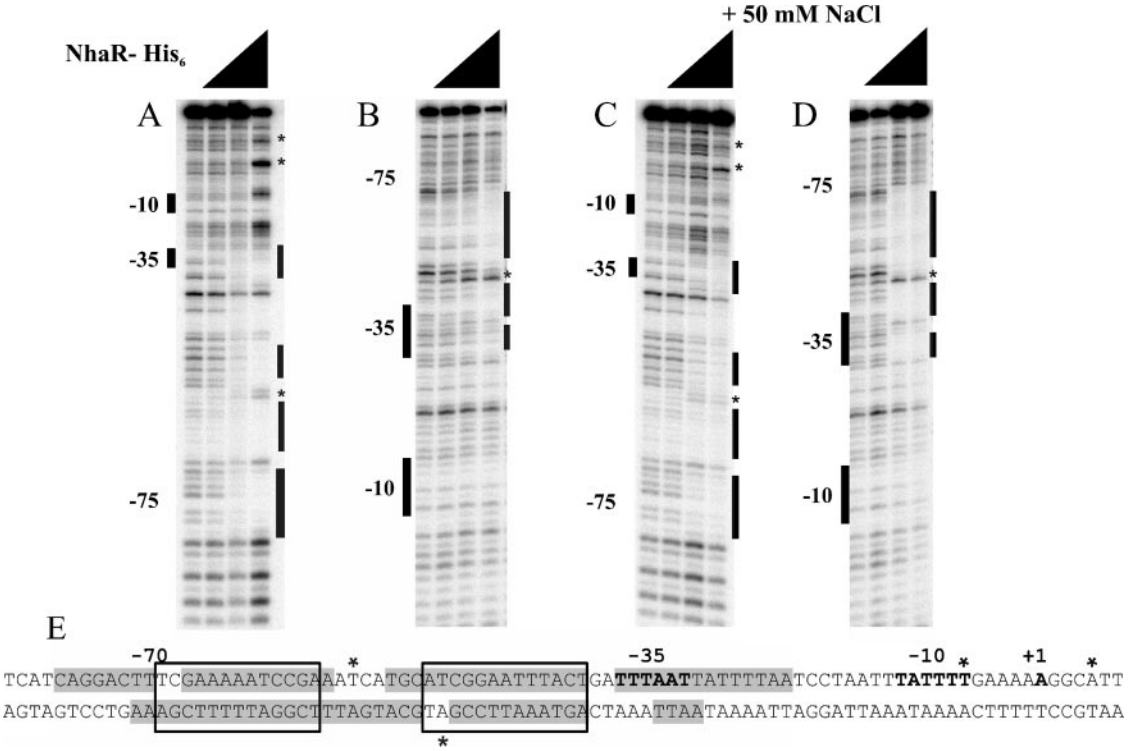

FIG. 6. DNase I protection footprint of NhaR on the *pgaA* promoter. A 132-bp PCR product containing the promoter region of *pgaA* (−115 to +18) was 5′ end labeled with ^{32}P on the top (A and C) or bottom (B and D) strand, as diagrammed in panel E, and subjected to DNase I footprinting in the presence of increasing concentrations of NhaR-His$_6$ (0, 0.29, 0.57, and 1.14 μM). The binding reaction mixtures contained no NaCl (A and B) or 50 mM NaCl (C and D). Protected regions are marked by vertical lines adjacent to the sequences. Hypersensitive sites are indicated by asterisks. Numbers depict positions relative to the initiating nucleotide (+1). These footprints were repeated four times, with no significant difference in the protection pattern observed in the presence or absence of NaCl. (E) Summary of DNase I footprinting. Protected regions are shaded gray; boxed sequences contain a LysR-type transcriptional regulator binding motif (T-N$_{11}$-A). The −35, −10, and +1 promoter elements are in boldface. Hypersensitive sites are indicated by asterisks.

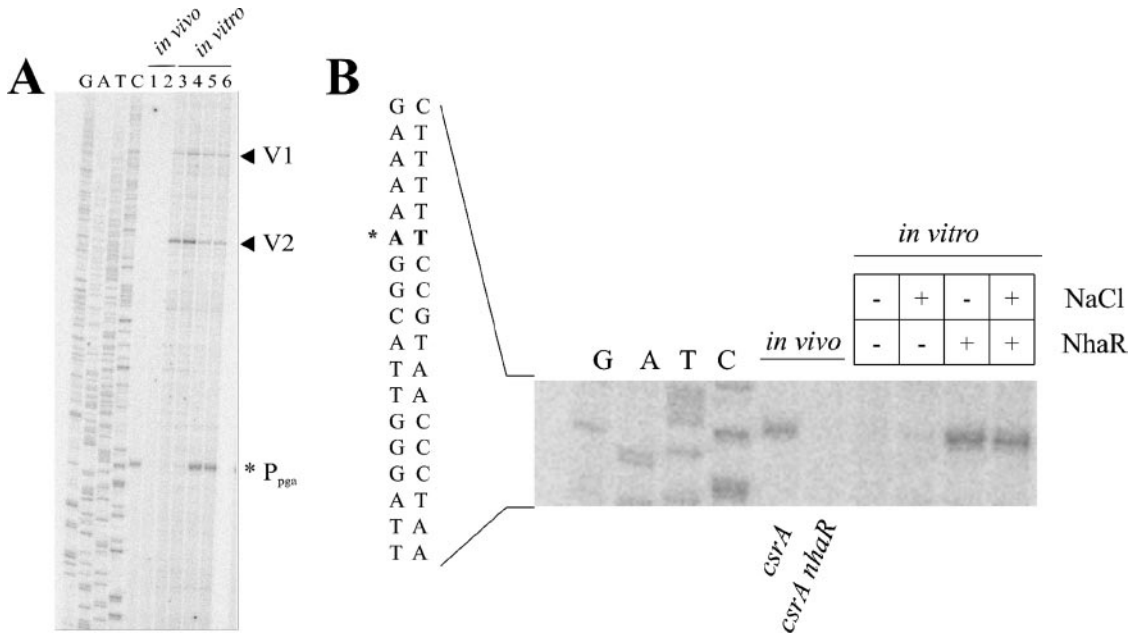

FIG. 7. NhaR-His$_6$ activates in vitro transcription from the *pgaA* promoter. NhaR-His$_6$ and σ^{70}-saturated RNA polymerase were used for in vitro transcription of plasmid DNA containing the *pgaABCD* operon (pPGA372). The resulting transcripts were analyzed by primer extension (see Materials and Methods). The full image (A) and a close-up (B) obtained from a single gel are shown. In the full gel image, two transcripts originating from the vector are indicated by arrowheads labeled V1 and V2; an asterisk denotes the 5′ end of the transcript originating from *pga* (P_{pga}). Identical results were obtained when 25 mM KCl was used instead of NaCl in the transcription reaction (data not shown). The first two lanes (in vivo) depict primer extension analysis of total cellular RNAs isolated from the indicated strains. The last four lanes (in vitro) correspond to transcription reactions conducted in the presence or absence of NhaR (455 nM) and NaCl (25 mM).

transcription of a *pgaABCD*-containing supercoiled plasmid template by σ^{70}-saturated *E. coli* RNA polymerase was determined in the presence or absence of NhaR-His$_6$. Recombinant NhaR was necessary and sufficient to activate in vitro transcription from the *pga* promoter (Fig. 7). The 5′ end of the NhaR-dependent in vitro transcript was identical to that observed in vivo. The intensities of two transcripts originating from vector DNA (V1 and V2) did not increase in the presence of NhaR (Fig. 7A). This indicates that NhaR was not acting as a general activator of transcription. Addition of 25 mM NaCl or KCl did not affect these reactions (Fig. 7 and data not shown).

NhaR is conserved in the *Enterobacteriaceae*. BLAST analyses revealed that homologs of *nhaAR* are present in the genomic sequences of most *Enterobacteriaceae* (82% of total), including pathogens such as *E. coli* O157:H7 (99% NhaR identity), *Yersinia pestis* (79%), and *Erwinia carotovora* (77%), which also contain loci homologous to the *pgaABCD* operon of *E. coli* (77). The genes of the *pgaABCD* operon encode proteins necessary for the synthesis and possibly the subcellular localization of polymeric PGA to the cell envelope (77). This polymer promotes biofilm formation in *E. coli* and several other species (36, 40). Furthermore, PGA-like polysaccharides are important determinants of disease transmission and virulence in *Yersinia pestis* and staphylococci, respectively (cited in reference 77). Additional investigation will be required to determine whether these species, which inhabit distinctly different environmental niches than *E. coli* K-12, utilize similar strategies for regulating PGA production and biofilm formation in response to environmental cues.

Conclusions. The present study demonstrates that the LysR-type transcriptional regulator NhaR is necessary and sufficient to activate transcription from the *pgaABCD* promoter of *E. coli* K-12 (Fig. 7) and consequently activates PGA production (Fig. 2) and biofilm formation (Fig. 1). It is evident that NhaR activates expression of its target operons, *nhaAR*, *osmC*, and *pgaABCD*, as a coordinated response to elevated Na^+ and/or pH. Consequently, NhaR is required for survival under high concentrations of NaCl, high pH, and certain oxidative stresses (49, 70). While the full ramifications of our findings remain to be determined, the regulatory role of NhaR in adhesion and biofilm formation is consistent with the idea that biofilm formation itself provides protection against a variety of biological and chemical stresses (13–15, 17, 19) and further suggests that NhaR is a stress response regulator of substantial importance.

These studies also demonstrate that monovalent cation concentrations, distinct from osmolarity, can be an important regulatory cue for biofilm formation by a gram-negative bacterium (Fig. 1 and 3). Surprisingly, activation of *pga* in vitro transcription by NhaR did not require monovalent cations (Fig. 7). As LTTR proteins often bind to their DNA targets in the absence of coinducer ligands (11, 64, 71), it was not surprising that NhaR bound to *pga* promoter DNA without the addition of salts. Likewise, it was not unexpected to find that the DNase I footprint pattern of NhaR was not altered by the addition of salts (Fig. 6) (10, 23). It is tempting to suggest that NhaR might not bind directly to its coinducer cations but might function similarly to the LTTR protein GcvA. In this case, the binding of glycine to GcvR prevents this protein from interacting with

GcvA to block activation (26, 32). Further studies will be required to assess this or other mechanisms that could explain the discrepancy between in vitro and in vivo cation requirements of NhaR.

ACKNOWLEDGMENTS

We thank Dietrich Mack for providing the anti-PIA antiserum and *Staphylococcus epidermidis* strains, Etana Padan for *E. coli* NM81 (*nhaA*::*kan*), and Rebecca DesPlas for sequencing of the transposon insertion site and construction of pCRnhaAR. We are also grateful to F. H. Strobel of the Emory University Mass Spectrometry Center for assistance with MALDI-TOF mass spectrometry. We also thank June R. Scott and Philip N. Rather for critical reading of the manuscript.

These studies were funded in part by the National Institutes of Health (grant GM066794). C. Goller was supported by an NIH Kirschstein predoctoral fellowship (F31AI064131-02). The Emory University Mass Spectrometry Center is funded by NIH grant 1S10 RR 14645-01.

Kane Biotech, Inc., may develop applications related to the findings herein. T. Romeo serves as chief scientific advisor for, owns equity in, and may receive royalties from this company. The terms of this arrangement have been reviewed and approved by Emory University in accordance with its conflict-of-interest policies.

REFERENCES

1. **Adams, J. L., and R. J. McLean.** 1999. Impact of *rpoS* deletion on *Escherichia coli* biofilms. Appl. Environ. Microbiol. **65:**4285–4287.
2. **Agladze, K., D. Jackson, and T. Romeo.** 2003. Periodicity of cell attachment patterns during *Escherichia coli* biofilm development. J. Bacteriol. **185:**5632–5638.
3. **Agladze, K., X. Wang, and T. Romeo.** 2005. Spatial periodicity of *Escherichia coli* K-12 biofilm microstructure initiates during a reversible, polar attachment phase of development and requires the polysaccharide adhesin PGA. J. Bacteriol. **187:**8237–8246.
4. **Altschul, S. F., W. Gish, W. Miller, E. W. Myers, and D. J. Lipman.** 1990. Basic local alignment search tool. J. Mol. Biol. **215:**403–410.
5. **Atlung, T., and H. Ingmer.** 1997. H-NS: a modulator of environmentally regulated gene expression. Mol. Microbiol. **24:**7–17.
6. **Beloin, C., and J. M. Ghigo.** 2005. Finding gene-expression patterns in bacterial biofilms. Trends Microbiol. **13:**16–19.
7. **Blumer, C., A. Kleefeld, D. Lehnen, M. Heintz, U. Dobrindt, G. Nagy, K. Michaelis, L. Emody, T. Polen, R. Rachel, V. F. Wendisch, and G. Unden.** 2005. Regulation of type 1 fimbriae synthesis and biofilm formation by the transcriptional regulator LrhA of *Escherichia coli*. Microbiology **151:**3287–3298.
8. **Branda, S. S., S. Vik, L. Friedman, and R. Kolter.** 2005. Biofilms: the matrix revisited. Trends Microbiol. **13:**20–26.
9. **Caiazza, N. C., and G. A. O'Toole.** 2004. SadB is required for the transition from reversible to irreversible attachment during biofilm formation by *Pseudomonas aeruginosa* PA14. J. Bacteriol. **186:**4476–4485.
10. **Carmel, O., O. Rahav-Manor, N. Dover, B. Shaanan, and E. Padan.** 1997. The Na^+-specific interaction between the LysR-type regulator, NhaR, and the *nhaA* gene encoding the Na^+/H^+ antiporter of *Escherichia coli*. EMBO J. **16:**5922–5929.
11. **Chen, X. C., J. Feng, B. H. Hou, F. Q. Li, Q. Li, and G. F. Hong.** 2005. Modulating DNA bending affects NodD-mediated transcriptional control in *Rhizobium leguminosarum*. Nucleic Acids Res. **33:**2540–2548.
12. **Corona-Izquierdo, F. P., and J. Membrillo-Hernandez.** 2002. A mutation in *rpoS* enhances biofilm formation in *Escherichia coli* during exponential phase of growth. FEMS Microbiol. Lett. **211:**105–110.
13. **Costerton, J. W., Z. Lewandowski, D. E. Caldwell, D. R. Korber, and H. M. Lappin-Scott.** 1995. Microbial biofilms. Annu. Rev. Microbiol. **49:**711–745.
14. **Costerton, J. W., and P. S. Stewart.** 2001. Battling biofilms. Sci. Am. **285:**74–81.
15. **Costerton, J. W., P. S. Stewart, and E. P. Greenberg.** 1999. Bacterial biofilms: a common cause of persistent infections. Science **284:**1318–1322.
16. **Da Re, S., and J. M. Ghigo.** 2006. A CsgD-independent pathway for cellulose production and biofilm formation in *Escherichia coli*. J. Bacteriol. **188:**3073–3087.
17. **Davies, D.** 2003. Understanding biofilm resistance to antibacterial agents. Nat. Rev. Drug Discov. **2:**114–122.
18. **Domka, J., J. Lee, and T. K. Wood.** 2006. YliH (BssR) and YceP (BssS) regulate *Escherichia coli* K-12 biofilm formation by influencing cell signaling. Appl. Environ. Microbiol. **72:**2449–2459.
19. **Donlan, R. M., and J. W. Costerton.** 2002. Biofilms: survival mechanisms of clinically relevant microorganisms. Clin. Microbiol. Rev. **15:**167–193.
20. **Dorel, C., O. Vidal, C. Prigent-Combaret, I. Vallet, and P. Lejeune.** 1999. Involvement of the Cpx signal transduction pathway of *E. coli* in biofilm formation. FEMS Microbiol. Lett. **178:**169–175.
21. **Dorman, C. J.** 2004. H-NS: a universal regulator for a dynamic genome. Nat. Rev. Microbiol. **2:**391–400.
22. **Dover, N., C. F. Higgins, O. Carmel, A. Rimon, E. Pinner, and E. Padan.** 1996. Na^+-induced transcription of *nhaA*, which encodes an Na^+/H^+ antiporter in *Escherichia coli*, is positively regulated by *nhaR* and affected by *hns*. J. Bacteriol. **178:**6508–6517.
23. **Dover, N., and E. Padan.** 2001. Transcription of *nhaA*, the main Na^+/H^+ antiporter of *Escherichia coli*, is regulated by Na^+ and growth phase. J. Bacteriol. **183:**644–653.
24. **Fux, C. A., J. W. Costerton, P. S. Stewart, and P. Stoodley.** 2005. Survival strategies of infectious biofilms. Trends Microbiol. **13:**34–40.
25. **Ghigo, J. M.** 2003. Are there biofilm-specific physiological pathways beyond a reasonable doubt? Res. Microbiol. **154:**1–8.
26. **Ghrist, A. C., and G. V. Stauffer.** 1995. Characterization of the *Escherichia coli gcvR* gene encoding a negative regulator of *gcv* expression. J. Bacteriol. **177:**4980–4984.
27. **Gong, X., R. Tao, and Z. Li.** 2006. Quantification of RNA damage by reverse transcription polymerase chain reactions. Anal. Biochem. **357:**58–67.
28. **Gonzalez Barrios, A. F., R. Zuo, Y. Hashimoto, L. Yang, W. E. Bentley, and T. K. Wood.** 2006. Autoinducer 2 controls biofilm formation in *Escherichia coli* through a novel motility quorum-sensing regulator (MqsR, B3022). J. Bacteriol. **188:**305–316.
29. **Gutierrez, C., and J. C. Devedjian.** 1991. Osmotic induction of gene *osmC* expression in *Escherichia coli* K12. J. Mol. Biol. **220:**959–973.
30. **Hall-Stoodley, L., J. W. Costerton, and P. Stoodley.** 2004. Bacterial biofilms: from the natural environment to infectious diseases. Nat. Rev. Microbiol. **2:**95–108.
31. **Hall-Stoodley, L., and P. Stoodley.** 2005. Biofilm formation and dispersal and the transmission of human pathogens. Trends Microbiol. **13:**7–10.
32. **Heil, G., L. T. Stauffer, and G. V. Stauffer.** 2002. Glycine binds the transcriptional accessory protein GcvR to disrupt a GcvA/GcvR interaction and allow GcvA-mediated activation of the *Escherichia coli gcvTHP* operon. Microbiology **148:**2203–2214.
33. **Heilmann, C., O. Schweitzer, C. Gerke, N. Vanittanakom, D. Mack, and F. Gotz.** 1996. Molecular basis of intercellular adhesion in the biofilm-forming *Staphylococcus epidermidis*. Mol. Microbiol. **20:**1083–1091.
34. **Hinsa, S. M., M. Espinosa-Urgel, J. L. Ramos, and G. A. O'Toole.** 2003. Transition from reversible to irreversible attachment during biofilm formation by *Pseudomonas fluorescens* WCS365 requires an ABC transporter and a large secreted protein. Mol. Microbiol. **49:**905–918.
35. **Hryniewicz, M. M., and N. M. Kredich.** 1991. The *cysP* promoter of *Salmonella typhimurium*: characterization of two binding sites for CysB protein, studies of in vivo transcription initiation, and demonstration of the anti-inducer effects of thiosulfate. J. Bacteriol. **173:**5876–5886.
36. **Itoh, Y., X. Wang, B. J. Hinnebusch, J. F. Preston III, and T. Romeo.** 2005. Depolymerization of β-1,6-*N*-acetyl-D-glucosamine disrupts the integrity of diverse bacterial biofilms. J. Bacteriol. **187:**382–387.
37. **Jackson, D. W., J. W. Simecka, and T. Romeo.** 2002. Catabolite repression of *Escherichia coli* biofilm formation. J. Bacteriol. **184:**3406–3410.
38. **Jackson, D. W., K. Suzuki, L. Oakford, J. W. Simecka, M. E. Hart, and T. Romeo.** 2002. Biofilm formation and dispersal under the influence of the global regulator CsrA of *Escherichia coli*. J. Bacteriol. **184:**290–301.
39. **Jubelin, G., A. Vianney, C. Beloin, J. M. Ghigo, J. C. Lazzaroni, P. Lejeune, and C. Dorel.** 2005. CpxR/OmpR interplay regulates curli gene expression in response to osmolarity in *Escherichia coli*. J. Bacteriol. **187:**2038–2049.
40. **Kaplan, J. B., K. Velliyagounder, C. Ragunath, H. Rohde, D. Mack, J. K. M. Knobloch, and N. Ramasubbu.** 2004. Genes involved in the synthesis and degradation of matrix polysaccharide in *Actinobacillus actinomycetemcomitans* and *Actinobacillus pleuropneumoniae* biofilms. J. Bacteriol. **186:**8213–8220.
41. **Leaphart, A. B., D. K. Thompson, K. Huang, E. Alm, X. F. Wan, A. Arkin, S. D. Brown, L. Wu, T. Yan, X. Liu, G. S. Wickham, and J. Zhou.** 2006. Transcriptome profiling of *Shewanella oneidensis* gene expression following exposure to acidic and alkaline pH. J. Bacteriol. **188:**1633–1642.
42. **Lejeune, P.** 2003. Contamination of abiotic surfaces: what a colonizing bacterium sees and how to blur it. Trends Microbiol. **11:**179–184.
43. **Lesniak, J., W. A. Barton, and D. B. Nikolov.** 2003. Structural and functional features of the *Escherichia coli* hydroperoxide resistance protein OsmC. Protein Sci. **12:**2838–2843.
44. **Mah, T. F., and G. A. O'Toole.** 2001. Mechanisms of biofilm resistance to antimicrobial agents. Trends Microbiol. **9:**34–39.
45. **Miller, J. H.** 1972. Experiments in molecular genetics. Cold Spring Harbor Laboratory, Cold Spring Harbor, N.Y.
46. **Muraoka, S., R. Okumura, N. Ogawa, T. Nonaka, K. Miyashita, and T. Senda.** 2003. Crystal structure of a full-length LysR-type transcriptional regulator, CbnR: unusual combination of two subunit forms and molecular bases for causing and changing DNA bend. J. Mol. Biol. **328:**555–566.
47. **O'Toole, G., H. B. Kaplan, and R. Kolter.** 2000. Biofilm formation as microbial development. Annu. Rev. Microbiol. **54:**49–79.
48. **Otto, K., and T. J. Silhavy.** 2002. Surface sensing and adhesion of *Escherichia*

coli controlled by the Cpx-signaling pathway. Proc. Natl. Acad. Sci. USA **99:**2287–2292.
49. **Padan, E., and S. Schuldiner.** 1994. Molecular physiology of the Na^+/H^+ antiporter in *Escherichia coli*. J. Exp. Biol. **196:**443–456.
50. **Padan, E., M. Venturi, Y. Gerchman, and N. Dover.** 2001. Na^+/H^+ antiporters. Biochim. Biophys. Acta **1505:**144–157.
51. **Padan, E., D. Zilberstein, and S. Schuldiner.** 1981. pH homeostasis in bacteria. Biochim. Biophys. Acta **650:**151–166.
52. **Parsek, M. R., and E. P. Greenberg.** 2005. Sociomicrobiology: the connections between quorum sensing and biofilms. Trends Microbiol. **13:**27–33.
53. **Pratt, L. A., and R. Kolter.** 1998. Genetic analysis of *Escherichia coli* biofilm formation: roles of flagella, motility, chemotaxis and type I pili. Mol. Microbiol. **30:**285–293.
54. **Prigent-Combaret, C., E. Brombacher, O. Vidal, A. Ambert, P. Lejeune, P. Landini, and C. Dorel.** 2001. Complex regulatory network controls initial adhesion and biofilm formation in *Escherichia coli* via regulation of the *csgD* gene. J. Bacteriol. **183:**7213–7223.
55. **Prigent-Combaret, C., G. Prensier, T. T. Le Thi, O. Vidal, P. Lejeune, and C. Dorel.** 2000. Developmental pathway for biofilm formation in curli-producing *Escherichia coli* strains: role of flagella, curli and colanic acid. Environ. Microbiol. **2:**450–464.
56. **Prigent-Combaret, C., O. Vidal, C. Dorel, and P. Lejeune.** 1999. Abiotic surface sensing and biofilm-dependent regulation of gene expression in *Escherichia coli*. J. Bacteriol. **181:**5993–6002.
57. **Rahav-Manor, O., O. Carmel, R. Karpel, D. Taglicht, G. Glaser, S. Schuldiner, and E. Padan.** 1992. NhaR, a protein homologous to a family of bacterial regulatory proteins (LysR), regulates *nhaA*, the sodium proton antiporter gene in *Escherichia coli*. J. Biol. Chem. **267:**10433–10438.
58. **Reisner, A., J. A. Haagensen, M. A. Schembri, E. L. Zechner, and S. Molin.** 2003. Development and maturation of *Escherichia coli* K-12 biofilms. Mol. Microbiol. **48:**933–946.
59. **Romeo, T.** 1998. Global regulation by the small RNA-binding protein CsrA and the non-coding RNA molecule CsrB. Mol. Microbiol. **29:**1321–1330.
60. **Romeo, T., J. Black, and J. Preiss.** 1990. Genetic regulation of glycogen biosynthesis in *Escherichia coli*: *in vitro* effects of catabolite repression and stringent response systems in *glg* gene expression. Curr. Microbiol. **21:**131–137.
61. **Romeo, T., M. Gong, M. Y. Liu, and A. M. Brun-Zinkernagel.** 1993. Identification and molecular characterization of *csrA*, a pleiotropic gene from *Escherichia coli* that affects glycogen biosynthesis, gluconeogenesis, cell size, and surface properties. J. Bacteriol. **175:**4744–4755.
62. **Rupp, M. E., J. S. Ulphani, P. D. Fey, K. Bartscht, and D. Mack.** 1999. Characterization of the importance of polysaccharide intercellular adhesin/hemagglutinin of *Staphylococcus epidermidis* in the pathogenesis of biomaterial-based infection in a mouse foreign body infection model. Infect. Immun. **67:**2627–2632.
63. **Sambrook, J., E. F. Fritsch, and T. Maniatis.** 1989. Molecular cloning: a laboratory manual, 2nd ed. Cold Spring Harbor Laboratory, Cold Spring Harbor, N.Y.
64. **Schell, M. A.** 1993. Molecular biology of the LysR family of transcriptional regulators. Annu. Rev. Microbiol. **47:**597–626.
65. **Smith, P. K., R. I. Krohn, G. T. Hermanson, A. K. Mallia, F. H. Gartner, M. D. Provenzano, E. K. Fujimoto, N. M. Goeke, B. J. Olson, and D. C. Klenk.** 1985. Measurement of protein using bicinchoninic acid. Anal. Biochem. **150:**76–85.
66. **Sorensen, S. J., M. Bailey, L. H. Hansen, N. Kroer, and S. Wuertz.** 2005. Studying plasmid horizontal transfer *in situ*: a critical review. Nat. Rev. Microbiol. **3:**700–710.
67. **Stanley, N. R., and B. A. Lazazzera.** 2004. Environmental signals and regulatory pathways that influence biofilm formation. Mol. Microbiol. **52:**917–924.
68. **Sturny, R., K. Cam, C. Gutierrez, and A. Conter.** 2003. NhaR and RcsB independently regulate the *osmC*p1 promoter of *Escherichia coli* at overlapping regulatory sites. J. Bacteriol. **185:**4298–4304.
69. **Suzuki, K., X. Wang, T. Weilbacher, A. K. Pernestig, O. Melefors, D. Georgellis, P. Babitzke, and T. Romeo.** 2002. Regulatory circuitry of the CsrA/CsrB and BarA/UvrY systems of *Escherichia coli*. J. Bacteriol. **184:**5130–5140.
70. **Toesca, I., C. Perard, J. Bouvier, C. Gutierrez, and A. Conter.** 2001. The transcriptional activator NhaR is responsible for the osmotic induction of *osmC*(p1), a promoter of the stress-inducible gene *osmC* in *Escherichia coli*. Microbiology **147:**2795–2803.
71. **Toledano, M. B., I. Kullik, F. Trinh, P. T. Baird, T. D. Schneider, and G. Storz.** 1994. Redox-dependent shift of OxyR-DNA contacts along an extended DNA-binding site: a mechanism for differential promoter selection. Cell **78:**897–909.
72. **Tropel, D., and J. R. van der Meer.** 2004. Bacterial transcriptional regulators for degradation pathways of aromatic compounds. Microbiol. Mol. Biol. Rev. **68:**474–500.
73. **Tyrrell, R., K. H. Verschueren, E. J. Dodson, G. N. Murshudov, C. Addy, and A. J. Wilkinson.** 1997. The structure of the cofactor-binding fragment of the LysR family member, CysB: a familiar fold with a surprising subunit arrangement. Structure **5:**1017–1032.
74. **Vidal, O., R. Longin, C. Prigent-Combaret, C. Dorel, M. Hooreman, and P. Lejeune.** 1998. Isolation of an *Escherichia coli* K-12 mutant strain able to form biofilms on inert surfaces: involvement of a new *ompR* allele that increases curli expression. J. Bacteriol. **180:**2442–2449.
75. **Wang, L., and S. C. Winans.** 1995. The sixty nucleotide OccR operator contains a subsite essential and sufficient for OccR binding and a second subsite required for ligand-responsive DNA bending. J. Mol. Biol. **253:**691–702.
76. **Wang, X., A. K. Dubey, K. Suzuki, C. S. Baker, P. Babitzke, and T. Romeo.** 2005. CsrA post-transcriptionally represses *pgaABCD*, responsible for synthesis of a biofilm polysaccharide adhesin of *Escherichia coli*. Mol. Microbiol. **56:**1648–1663.
77. **Wang, X., J. F. Preston III, and T. Romeo.** 2004. The *pgaABCD* locus of *Escherichia coli* promotes the synthesis of a polysaccharide adhesin required for biofilm formation. J. Bacteriol. **186:**2724–2734.
78. **Wood, T. K., A. F. Gonzalez Barrios, M. Herzberg, and J. Lee.** 2006. Motility influences biofilm architecture in *Escherichia coli*. Appl. Microbiol. Biotechnol. **72:**361–367.
79. **Yakhnin, A. V., J. J. Trimble, C. R. Chiaro, and P. Babitzke.** 2000. Effects of mutations in the L-tryptophan binding pocket of the Trp RNA-binding attenuation protein of *Bacillus subtilis*. J. Biol. Chem. **275:**4519–4524.
80. **Zogaj, X., M. Nimtz, M. Rohde, W. Bokranz, and U. Romling.** 2001. The multicellular morphotypes of *Salmonella typhimurium* and *Escherichia coli* produce cellulose as the second component of the extracellular matrix. Mol. Microbiol. **39:**1452–1463.